Thermochimica Acta 664 (2018) 108–117

Contents lists available at ScienceDirect

Thermochimica Acta

journal homepage: www.elsevier.com/locate/tca

Hydration kinetics of cement incorporating different nanoparticles at elevated temperatures

Guangcheng Long, Yuanyuan Li, Cong Ma*, Youjun Xie, Ye Shi

School of Civil Engineering, Central South University, Changsha, 410075, PR China

ARTICLE INFO

Keywords:
Hydration heat
Kinetics model
Nanoparticles
Nucleation and growth processes
Elevated temperature

ABSTRACT

The nanometer materials and technology are becoming new ways for cementitious composite innovation due to the significant improvement of microstructure and mechanical performance of cement-based materials. In this study, the isothermal calorimetry was employed to measure the heat release rate and total heat release of multi-scale cement system incorporated with different nanoparticles at elevated temperatures. The nucleation and growth processes of hydration products were simulated through a kinetics model. It is discovered that the effects of nanoparticles on cement hydration depend on itself chemical reactivity and physical properties as well as ambient temperature. Both nano-SiO_2 and nano-C-S-H can obviously shorten the induction period of cement hydration and have acceleration effects obviously. Addition of 1% nano-$CaCO_3$ seems to have no obvious effect on cement hydration process at elevated temperatures. The acceleration effects of nano-particles mainly refer to the improvement of the nucleation rate of hydrates. Generally, the effect of nanoparticles on nucleation process is more significant than that on growth process. Nano-SiO_2 and nano-$CaCO_3$ have slight influence on the growth rate, but the nano-C-S-H can increase the growth rates to some extent at different temperatures.

1. Introduction

Elevated temperature curing conditions, such as steam curing and autoclaved curing, are commonly employed in the production of large-scale precast elements including the key components of the ballastless track slab and simply-supported prestressed concrete box-girder of high-speed railway in China. Under elevated temperature condition, concrete can rapidly gain high early strength without the requirement of other external chemical agents. The turnaround efficiency of the moulds and the construction progress of the corresponding precast concrete elements can be thus highly enhanced [3]. Of course, the performance of concrete at elevated temperature condition and thus the precast concrete element is the core concerned focus by researchers, constructer and managers, which involves the long-term quality and safety of huge engineering structures including the high-speed railway of more than forty thousand kilometer in predictable future [1,2,4].

However, some common deficiencies, such as higher brittleness and more poor durability are found in the steam-cured concrete components, rather than the concrete structures cured at standard condition. It is quite logical to realize that the deficiencies in concrete structures can affect the normal operation of high-speed railway. The ordinary method applied to solve the defect of steam-cured concrete in China is adding some supplementary cementitious materials (SCMs), such as fly ash, GGBS and silica fume [5–9]. The mechanisms of SCMs on hydration kinetics of cement were studied by many researchers, and many interesting results were reported [10–13]. For example, fly ash was proved to retard the cement hydration during the early term and accelerate the cement hydration at the later term when the curing temperature is lower than 50 °C [11]. Even so, it is no doubt that the elevated temperature promotes cement hydration even though the SCMs contents are relatively high.

In comparison to the micro-scale SCMs, some nano materials or nanoparticles, such as nano-silica (nano-SiO_2), nano-alumina (nano-Al_2O_3) and nano-C-S-H, were proved to be more effective to enhance the performances of cement-based materials [14–19]. Nano-SiO_2 performs chemical reactions with calcium hydroxide and the pozzolanic effect is more effective than traditional SCMs. In addition the crystal dimension of portlandite(CH) crystals distributing in the interfacial transition zone (ITZ) is also reduced, which results in the improvement of the ITZ performance. It is interesting that nano-C-S-H promotes the cement hydration, as indicated by heat release rate, with the decrease in total hydration heat. It is also critical to note that the appropriate addition of nanoparticles ranges from 0.25% to 5% while excessive nanoparticles have the opposite effects [15]. Moreover, the simultaneous use of two or three nanoparticles may be superior to the single nanoparticle [19].

* Corresponding author.
E-mail address: macgyh090@csu.edu.cn (C. Ma).

https://doi.org/10.1016/j.tca.2018.04.017
Received 1 March 2018; Received in revised form 22 April 2018; Accepted 30 April 2018
Available online 01 May 2018
0040-6031/

Nomenclature

CH	portlandite
g	degree of anisotropy of the growth rate
G	growth rate of nuclei (um/h)
ITZ	interfacial transition zone
k	rates of nucleation and growth processes of hydration products
k_G	growing time of hydration products reaching to the radius of the "reaction vessel" (h^{-1})
k_N	$1/kN^{1/3}$ is the needed time for part of hydration products along the boundary of cement particles to become unity (h^{-3})
N	nucleation rate of nuclei ($um^{-2}h^{-1}$)
SCM	supplementary cementitious material
t	time (h)
X	hydration degree
y	a dummy variable

It clearly appears that most nanoparticles can accelerate the cement hydration through providing more nucleation sites. After the dissolution of cement particles in water, the formation process of hydration products is divided into three steps: nucleation and crystal growth, interactions at phase boundaries and diffusion. The hydration products covering on cement particles may hinder the latter two processes, especially at elevated temperatures. Because the nanoparticles have huge surface areas, they can provide many nucleation sites, which may influence the nucleation and growth processes of hydration products. In addition, the effects of nanoparticles on cement hydration may be magnified under elevated temperature conditions. However, there are few studies on the hydration kinetics of cement-based materials containing nanoparticles at elevated temperatures.

In this study, three types of nanoparticles were employed to prepare cement-based materials. The influences of nanoparticles on cement hydration at different temperatures were explored through the isothermal calorimetry. Cahn's hydration kinetics model is used to analyze the hydration kinetics of cement-based materials. The key parameters controlling the hydration kinetics are obtained from the analysis results. Silica fume used as SCM is compared with nanoparticles. This research not only gives a perspective on the hydration kinetics of nanoparticles modified cement system at elevated temperatures, but also discusses the difference in the influences of nanoparticles and microparticles on the hydration kinetics.

2. Hydration kinetic model

As mentioned above, the hydration process of cement is very complicated, which involves physicochemical interaction between cement clinker and water, such as dissolution, nucleation, diffusion and etc. Many scientists have made much effort to explain the process of hydration kinetics and established corresponding models. The classical JMAK model considered that the cement hydration nucleation occurs randomly ieqn the system and it was written as Eq. (1) [20].

$$-\ln(1-X) = kt^n \tag{1}$$

where X is the hydration degree, k is an invariant representing the rates of nucleation and growth processes, t is time. Several researchers proposed the modified JMAK models for cement-based materials with SCMs. Considering the nucleation mainly occurring on particle surface, Cahn's nucleation model was proposed as the following equation [21].

$$X = 1 - \exp\left\{-S\int_0^{Gt}\left[1-\exp\left(\frac{-\pi N}{3}G^2t^3\left(1-\frac{3y^2}{G^2t^2}+\frac{2y^3}{G^3t^3}\right)\right)\right]dy\right\} \tag{2}$$

where S is the value of surface area for the solid particles per unit volume, G is the growth rate of nuclei, N is the producing rate of nuclei and y is a dummy variable. This nucleation model was employed for analyzing the hydration kinetics of cement or cement admixed with SCMs. As mentioned before, nanoparticles can provide abundant nucleation sites, which seems like the role of cement clinker. Hence, the Cahn's nucleation model is appropriate to describe the nucleation and growth rates of hydration products in nanoparticles modified cement. And the nucleation rate (N) and growth rate (G) are both dominant parameters controlling the early-term cement hydration. Because the nuclei growth is anisotropic, the rate of tangent direction can be defined as gG. In addition a parameter p is proposed in order to represent the proportion of growth rates inside and outside the cement clinker. And by defining $u = y/(G{\cdot}t)$, the hydration degree can also be written as [22,23]:

$$X = 1 - \exp\left\{-2pSGt\int_0^1\left[1-\exp\left(\frac{-\pi N}{3}gG^2t^3(1-u)^2(1+2u)\right)\right]du\right\},\ u<1 \tag{3}$$

Further, in order to achieve the simplification of the above equation, another two constants are defined as follows.

$$k_G = pSG \tag{4}$$

$$k_N = \pi gG^2N/3 \tag{5}$$

The reciprocal of k_G is the growing time of hydration products reaching to the radius of the "reaction vessel". Likewise, the $1/k_N^{1/3}$ is the needed time for part of hydration products along the boundary of cement particles to become unity [22]. With the combination of three Eqs. (3)–(5), the hydration degree can be expressed as the following formula.

$$X = 1 - \exp\left\{-2k_Gt\int_0^1\left[1-\exp(-k_Nt^3(1-u)^2(1+2u))\right]du\right\},\ u<1 \tag{6}$$

This study employs Eq. (6) to simulate the hydration kinetics of nanoparticles modified cement system at different temperatures.

Table 1
Chemical composition of used materials.

Materials	Mass fraction (%)							Average size(nm)	Specific surface area (m^2/kg)	LOI (%)
	SiO_2	Al_2O_3	Fe_2O_3	CaO	MgO	SO_3	f-CaO			
PC	20.76	7.31	3.25	62.26	2.91	2.81	0.7	20000	354	2.1
SF	93	0.4	0.8	0.6	0.6	0.4	–	120	17800	3.9
Nano-$CaCO_3$	–	–	–	55.7	–	–	–	50	40000	
Nano-SiO_2	99.5	–	–	–	–	–	–	30	150000	
Nano-C-S-H	–	–	–	–	–	–	–	–	180000	

3. Experimental methodology

3.1. Materials

Each experiment in this study employs CEM 42.5R Portland cement (PC) whose oxide compositions are presented in Table 1. Silica fume (SF) used as a typical SCM is obtained from Elkem Carbon (China) Company limited, and its apparent density is 2.1 g/cm^3. The oxide composition of silica fume is presented in Table 1. Three types of nanoparticles are employed, and they are nano-$CaCO_3$ particle, nano-SiO_2 particle and nano-C-S-H (solution) with a concentration of 20% by commercially available. The specific surface areas of the nanoparticles are also shown in Table 1. The structures of nano-$CaCO_3$ and nano-SiO_2 obtained via transmission electron microscope (TEM) are presented in Fig. 1. The nano-C-S-H used is synthesized and polymerized in aqueous solution, and the molar ratio of nano-C-S-H is 0.88. The amorphous nano-C-S-H used in solution is poor crystallization.

3.2. Experimental method

The mix proportion used in the experiments was designed as Table 2. The water to binder ratio (w/b) is fixed at 0.3 for each specimen. MIX CON is the contrast specimen containing only cement. MIX CSF is the specimen containing cement and single SCM and designed to compare with specimens with nanoparticles including CNC, CNS and CNCSH as shown in Table 2.

An in-situ isothermal calorimeter named as TAM Air is employed to conduct isothermal calorimetry tests. The twin-chamber testing channel is the typical characteristics of this apparatus, and one contains the distilled water and the other contains the predetermined amount of slurry. The TAM Air apparatus was adjusted to the measurement temperatures (from 40 °C to 70 °C) before sample preparation. The fresh paste for each experiment was mixed under environmental conditions similar with the measurement conditions in order to eliminate the possible experimental error. After mixing homogeneously, the slurry was immediately transferred into the apparatus. The testing time lasted from the induction period to the end of the main hydration heat evolution peak until the hydration tended to be stable.

4. Results and discussion

4.1. The characterization of heat release during early-term hydration process

The heat release rate and accumulated heat release of different pastes measured at 40 °C are shown in Fig. 2. It is noteworthy that there are two remarkable peaks of heat release rate in Fig. 2(a). The first peak appearing immediately after mixing is the heat release of rapid dissolution of cement particles in slurry, and the following decrease in heat release rate is known as induction period. The heat release in the initial dissolution and induction periods is only five percent in the total heat release of cement hydration. Thus the following rapid acceleration period, as indicated by the second peak of heat release rate, is central to the hydration degree of cement and nucleation and growth processes of hydrates. After induction process, the alite particles begin to dissolve and perform chemical reactions. The hydration products nucleate and grow quickly on the surface of alite particles. As the retardation of gypsum gradually becomes failure, water can permeate through the adsorption layer and more alite particles can participate in the hydration. These could explain the two exothermic effects during acceleration period at 40 °C. An interesting founding is that an inconspicuous flat hump is observed between about 12.5 h and 15 h during deceleration period. The phase transformation of unstable ettringite (AFt) to stable monosulphate (AFm) can explain this phenomenon [24]. Although the silica fume and nano-SiO_2 can shorten the induction period, the values of maximal heat release rate decrease slightly. Nano-C-S-H significantly increases the maximal heat release rate which is 32.7% higher than the maximal heat release rate of MIX CON. The possible reason may be that the addition of C-S-H seeds make the hydration products nucleate on the grain surface and the C-S-H seed region, which accelerates the rate of early hydration. It also clearly appears that the heat release rate of MIX CNCSH in steady state period is much lower than other mixtures, which results in the small difference in 20-hour cumulative heat [Fig. 1(b)].

Fig. 3 presents the heat release rate and cumulative heat of different pastes measured at 50 °C. It is no doubt that the maximal heat release rate increases significantly at 50 °C, thereby increasing the early-term cumulative heat. It is observed that the second peaks in Fig. 3(a) become much narrower in comparison to those in Fig. 2(a). The effects of silica fume and nano-SiO_2 on heat release rate of cement hydration at 50 °C are almost the same as that at 40 °C. It is noteworthy that the usage of nano-SiO_2 decreases the rapid acceleration of second peaks to a certain extent and increases the 20 h cumulative heat slightly [Fig. 3(b)]. The induction period of specimens with nano-$CaCO_3$ slightly shortens in comparison to MIX CON, and the maximal heat release rate and 20-hour cumulative heat also change. The maximal

Table 2
Mix proportion.

MIX ID.	Binder (%)					w/b
	cement	SF	Nano-$CaCO_3$	Nano-SiO_2	Nano-C-S-H	
CON	100	0	0	0	0	0.3
CSF	99	1	0	0	0	0.3
CNC	99	0	1	0	0	0.3
CNS	99	0	0	1	0	0.3
CNCSH	99	0	0	0	1	0.3

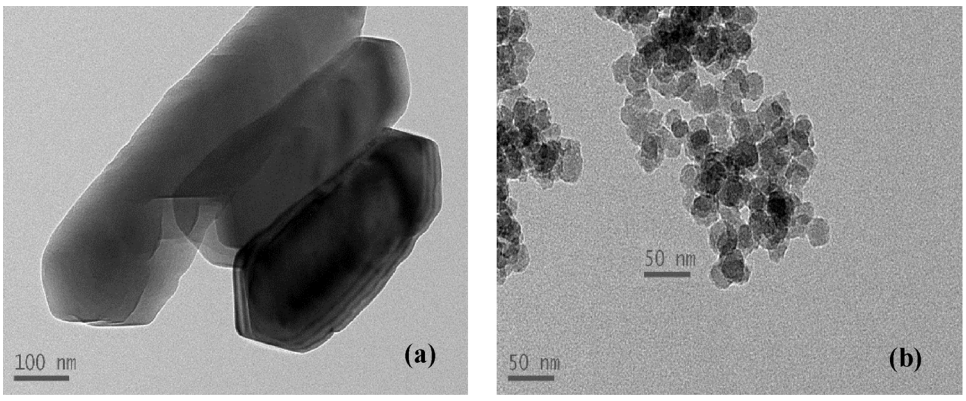

Fig. 1. TEM photos of nano-$CaCO_3$ (a) and nano-SiO_2 (b).

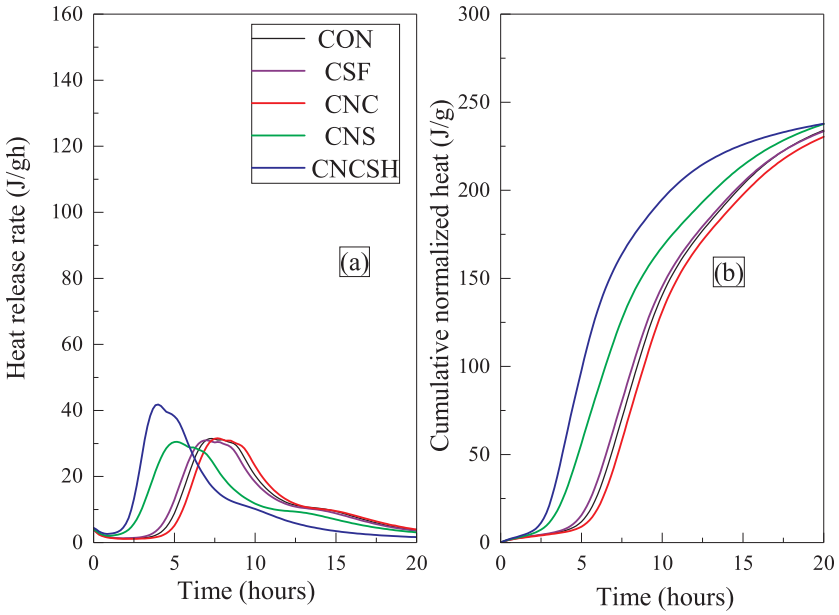

Fig. 2. Heat release rate and cumulative heat of different pastes measured at 40 °C.

heat release rate of nano-C-S-H modified cement is 62.80 J/gh, which is 24.7% higher than that of MIX CON at 50 °C. The heat release rate of MIX CNCSH decreases sharply during deceleration period and its value in steady state period is also much lower than other mixtures. In addition the 20 h cumulative heat of MIX CNCSH is the lowest.

The heat release rate and cumulative hydration heat of different pastes measured at 60 °C and 70 °C are presented in Figs. 4 and 5. At 60 °C and 70 °C, the second peaks of heat release rate are sharp ones and the rapid acceleration period of each mixture finishes within 5 h. In comparison to the phenomenon observed under relatively lower temperatures, there is only one exothermic effect at 60 °C and 70 °C. The possible reason may be that the gypsum loses the retardation efficacy much earlier and more alite particles participate in hydration under higher temperature condition. The silica fume, nano-SiO_2 and nano-C-S-H obviously shorten the induction period at different degrees. The peak values of the heat release rate of MIXs CON, CSF and CNS are almost the same except specimens with nano-$CaCO_3$ and nano-C-S-H. The curved lines describing heat release rate and cumulative heat of binder with silica fume and nano-SiO_2 are almost coincident as shown in Fig. 4(a). This may indicate that the roles of silica fume and nano-SiO_2 in cement paste are almost the same at 60 °C. As demonstrated in Fig. 5(a), the maximum value of heat release rate increases significantly, and the second peaks become sharper with the curing temperature rising to 70 °C. At this point, the nano-$CaCO_3$ has little influence on the cement hydration because the hydration release rate and cumulative exothermic curves of the nano-$CaCO_3$ system and the cement system are almost coincident. The maximal heat release rate of nano-C-S-H modified cement is 146.3 J/gh, which is 17.1% higher than that of MIX CON at 70 °C.

The arrival time of hydration heat release rate peak and the maximal heat release rate were shown in Fig. 6. It can be seen from Fig. 6(a) that when the temperature elevates from 40 °C to 70 °C, the arrival time of MIX CNC is fluctuant and almost the same as that of MIX CON while the ones for samples incorporating with 1% nano-SiO_2 and nano-C-S-H

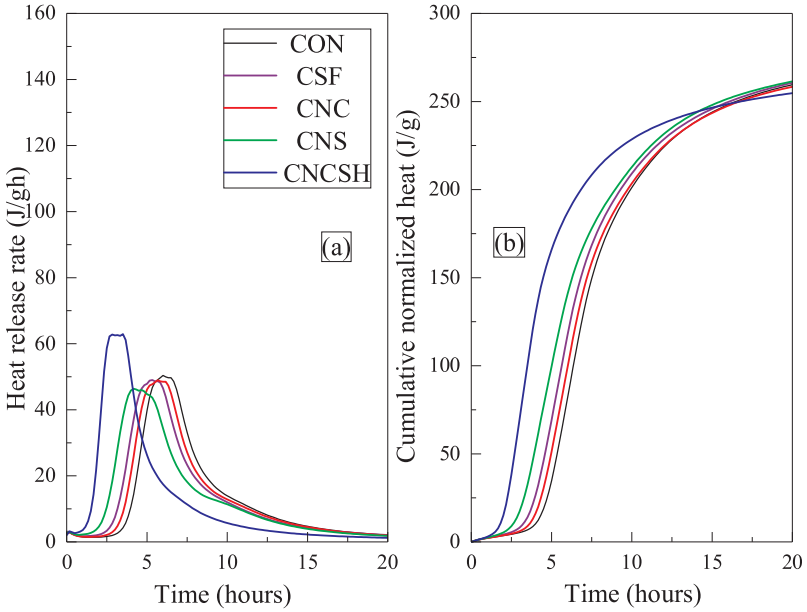

Fig. 3. Heat release rate and cumulative heat of different pastes measured at 50 °C.

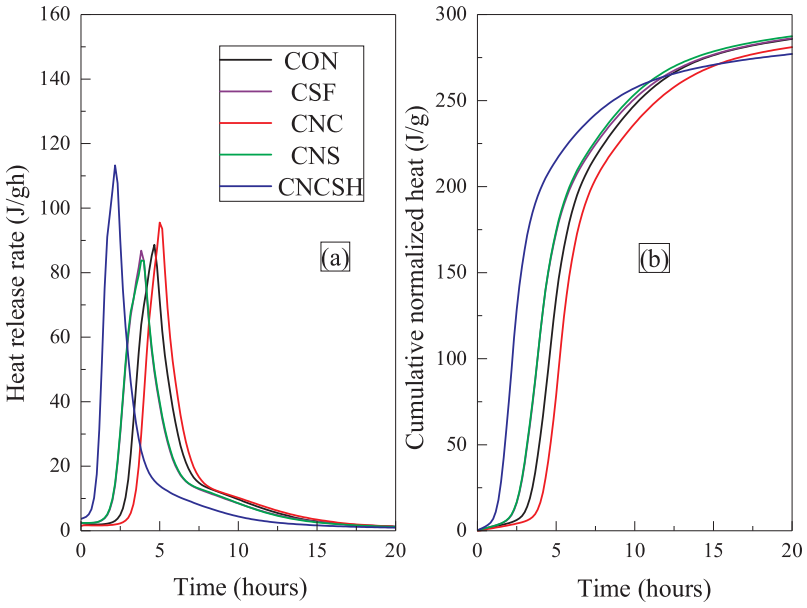

Fig. 4. Heat release rate and cumulative heat of different pastes measured at 60 °C.

are smaller than that of MIX CON. Especially for MIX CNSCH, the arrival time of heat release rate peak is significantly advanced. The peak value of hydration heat release rate of different specimens gradually increases at different levels with the temperature rising from 40 °C to 70 °C [Fig. 6(b)]. When the temperature rises from 40 °C to 70 °C, the peak values of MIXs CON, CSF, CNC, CNF and CNCSH increase by 297%, 285%, 292%, 289% and 249%, respectively. It is believed that the sensitivity of pure cement to temperature is the most remarkable, and that of nano-C-S-H modified cement is relatively lower.

The effects of different nanoparticles on cement hydration at elevated temperatures can be summarized as follows. Firstly, nano-SiO_2 and nano-C-S-H can shorten the induction period of cement hydration for each temperature regime. And the acceleration of nano-SiO_2 is more moderate than the effect of nano-C-S-H. Secondly, in comparison to the usage of nanoparticles, the influence of curing temperature on hydration is more significant. Thirdly, the early-term cumulative heat of cement with different nanoparticles changes a little, even though there is a great difference in the induction period and maximal heat release rate.

4.2. Simulation of the heat release of mixtures through a kinetics model

The above Eq. (6) can be employed to simulate the heat release rate and cumulative heat of cement pastes. The parameters indicating the nucleation and growth of hydrates could also be obtained by the Cahn's model. In the MATLAB computing process, the parameters in Cahn's model were adjusted automatically through a calculation procedure. The heat release rate and cumulative heat of cement pastes at elevated temperatures are shown in Figs. 7–10. In the curves of measured heat release rate of cement pastes, two peaks in acceleration period are

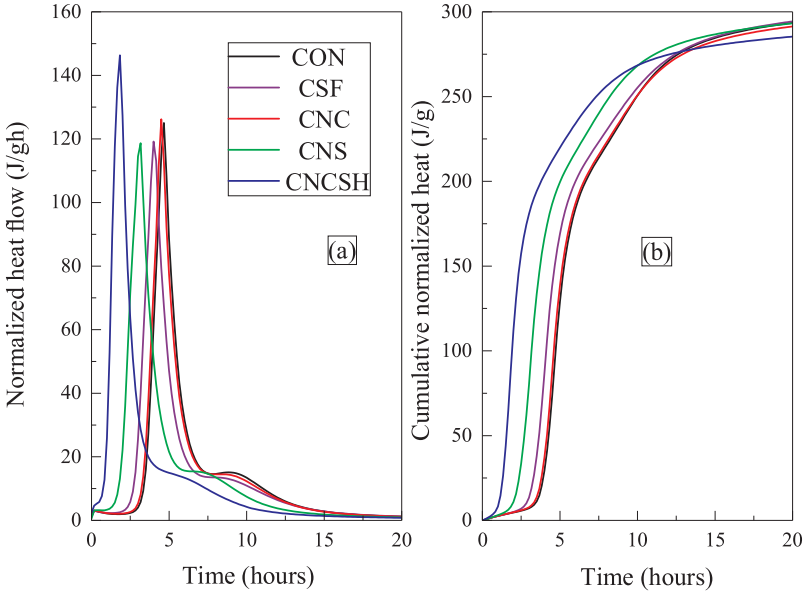

Fig. 5. Heat release rate and cumulative heat of different pastes measured at 70 °C.

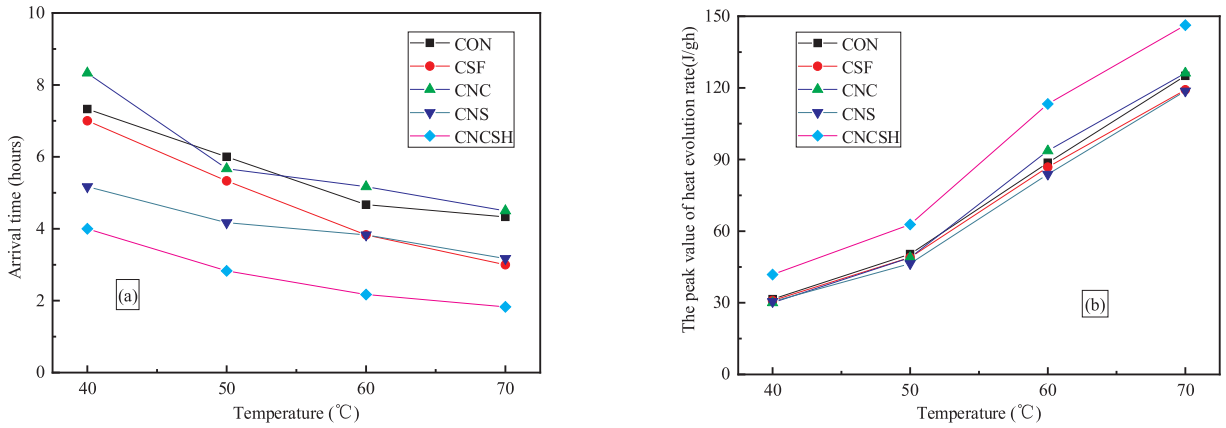

(a) Arrival time of heat release rate peak (b) Value of heat release rate peak

Fig. 6. The relationships of the arrival time and heat release rate peak to temperature. (a) Arrival time of heat release rate peak. (b) Value of heat release rate peak.

detected at 40 °C. This is because that although the hydration of tricalcium silicate is the controlling factor for the main peak, the generation of high-alumina phases during early term may be responsible for the nucleation process indicating as the should peak [25]. But the Cahn's model could only describe the second peak of the heat release rate. The simulated curves of heat release rate may be over or below the measured ones [Fig. 7(a)]. It is also observed in Fig. 6(a) that there is only a slight difference among the fitted heat release rates of specimens CON, CSF, CNC and CNS during the acceleration period. And the fitted heat release rates during the deceleration period are a little higher than the experimental results, which may explain the deviation between simulated results and measured cumulative heat observed in Fig. 7(b). Due to the acceleration effect, the early hydration product layer can hinder the penetration of water into the cement particles and influence the subsequent hydration of cement. Therefore, the diffusion-controlled process occurs earlier, and this may affect the accuracy of fitted results. When the curing temperature increases to 50 °C, some similar phenomena can be observed in Fig. 8 by comparing the fitted curves with the experimental results. The phenomenon of fitted heat release rates higher than measured ones during the deceleration period takes place at about 8 h as observed in Fig. 7(a), and the time of this phenomenon occurs much earlier with increasing the temperature from 40 °C to 70 °C [Fig. 10(a)]. This indicates that the temperature is also a critical factor for the fitted accuracy of the Cahn's model.

The two parameters k_N and k_G for each specimen at different temperatures can be obtained from the fitted curves, and the values of k_N and k_G are presented in Table 3. It is observed in Table 3 that the k_N values of MIX CSF at different temperatures are higher than those of MIX CON, and the k_N values of MIX CSF at 40 °C is about fifty percent higher than that of MIX CON. It is interesting there is only a slight difference among the k_G values of MIXs CSF and CON. That is to say, the influences of admixtures on nucleation process and growth process of hydration products may be inconsistent. The k_N and k_G values of MIXs CNS and CNCSH at different temperatures are greater than those of MIX CON, which illustrates the usage of nano-SiO_2 and Nano-C-S-H has different acceleration effects on cement hydration. The k_N values of MIX CNS at different temperatures are several times higher than those of MIX CON, but the difference in k_G values is inapparent. This confirms the above observation. And the relationships of two parameters k_N and k_G of different specimens with temperature are drawn and analyzed in

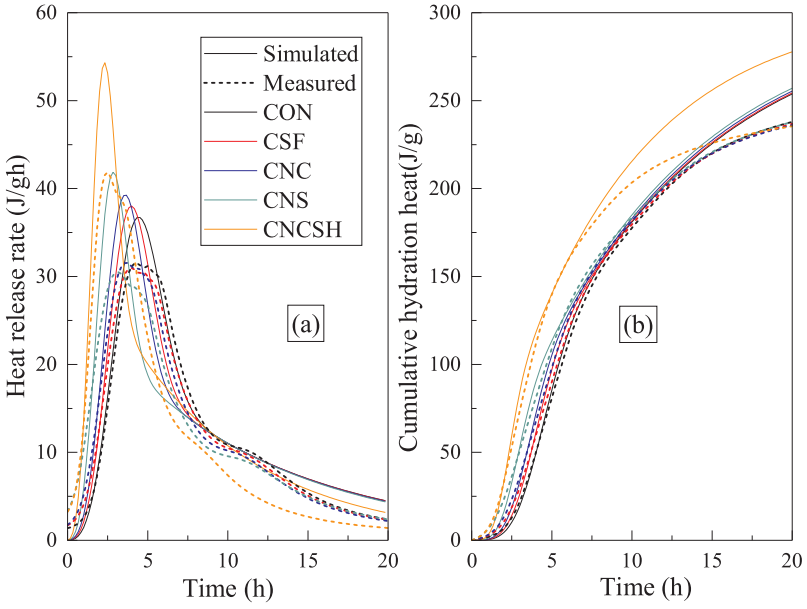

Fig. 7. Simulative curves from Eq. (6) for cement pastes at 40 °C.

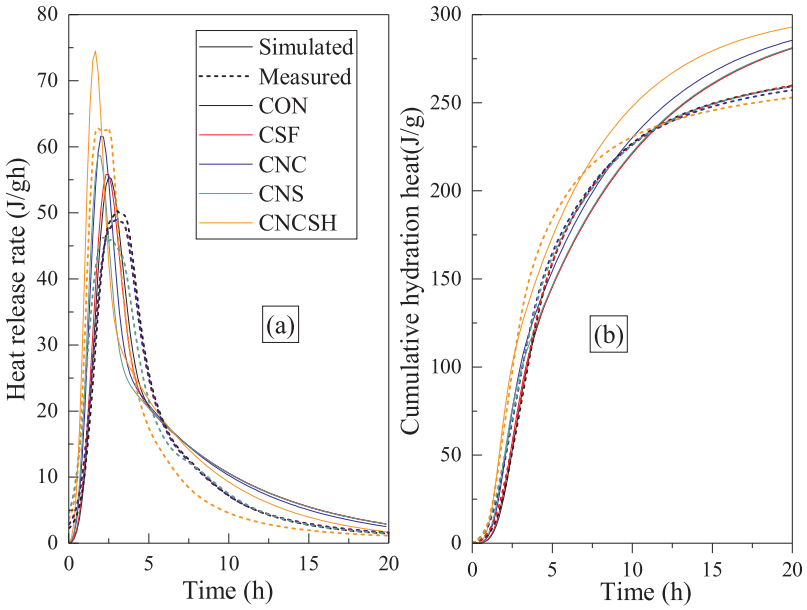

Fig. 8. Simulative curves from Eq. (6) for cement pastes at 50 °C.

Fig. 11 in order to understand the influence of temperature on the hydration kinetics clearly. The k_N and k_G values of MIX CNCSH are highest at different temperatures, which confirms that the addition of nano-C-S-H has the greatest effect on hydration kinetics of cement paste. Nano-C-S-H has the most significant effect on nucleation and growth rates of hydration products, followed by nano- SiO_2, and followed by nano-$CaCO_3$. It is no doubt that the k_N and k_G values increase significantly with increasing the temperature from 40 °C to 60 °C. Although there is an unexpected increase in k_N value of MIX CNCSH at 50 to 60 °C, the relationship of k_G value to temperature may agree with linear model. It is noteworthy that the k_N and k_G values increase slightly with temperature increases from 60 °C to 70 °C.

Based on the fitted results presented in Table 3, the parameters N and G which could be calculated through Eqs. (4) and (5) can describe the measured nucleation and growth rates more intuitively. The calculated N and G values are presented in Table 4. The tendency of N and G of different specimens is similar to that presented in the parameters k_N and k_G. The usage of silica fume, nano-SiO_2 and Nano-C-S-H increases the nucleation rate at different levels, and nano-$CaCO_3$ has little effect on the nucleation rate. This observation proves that the silica fume and nanoparticles can provide nucleation sites. Except MIX CNCSH, the difference in growth rates of different specimens at different temperatures is very small. This implies that Nano-C-S-H can accelerate both the nucleation rate and growth rate of hydration products. The relationship of N and G with temperature for different specimens are presented in Fig. 12. The nucleation rate and growth rate increase with the increasing temperature. The nucleation rate of MIX CNCSH at 70 °C is 38.1083 um^{-2}/h, which is almost fifty percent higher than that at 60 °C. And the growth rate of MIX CNCSH at 70 °C is 0.1096 um/h, which is only 18% higher than that at 60 °C. This implies that the increase rate of nucleation rate is much greater than that of growth rate when the temperature increases from 60 °C to 70 °C. The nucleation rates of cement with nano-C-S-H and nano-SiO_2 at 40 °C and 50 °C are much higher than those of other specimens. As the

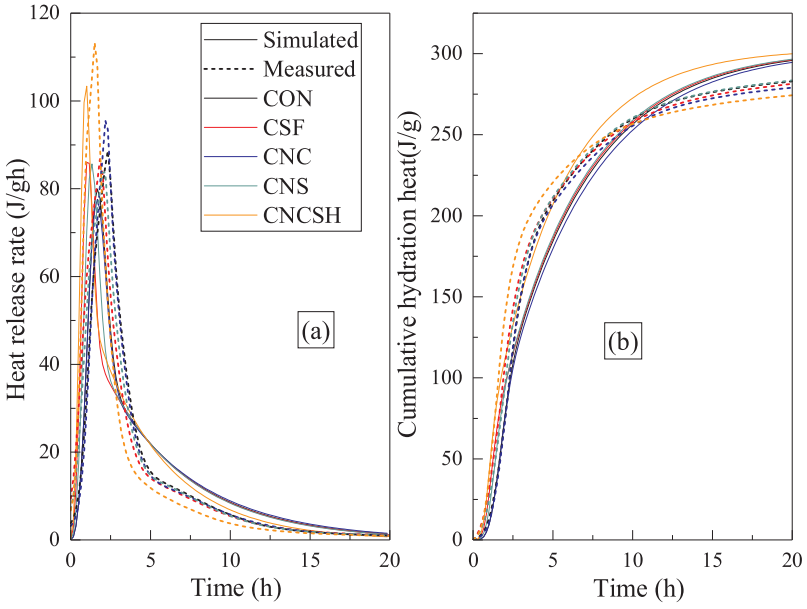

Fig. 9. Simulative curves from Eq. (6) for cement pastes at 60 °C.

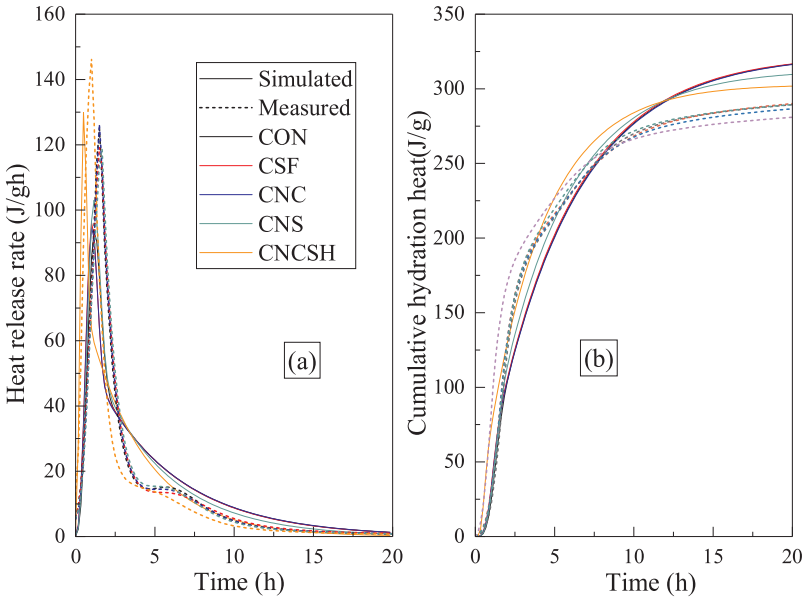

Fig. 10. Simulative curves from Eq. (6) for cement pastes at 70 °C.

Table 3
Fitted parameters obtained from fitted curves.

Temperature (°C)	Parameter	CON	CSF	CNC	CNS	CNCSH
40	$k_N(h^{-3})$	0.0041	0.0061	0.0037	0.0116	0.0259
	$k_G(h^{-1})$	0.0388	0.0391	0.0375	0.0411	0.0539
50	$k_N(h^{-3})$	0.0073	0.0122	0.0086	0.0208	0.0789
	$k_G(h^{-1})$	0.0515	0.0535	0.0563	0.0549	0.0742
60	$k_N(h^{-3})$	0.0188	0.0392	0.0136	0.0382	0.3330
	$k_G(h^{-1})$	0.0734	0.0767	0.0667	0.0721	0.1029
70	$k_N(h^{-3})$	0.0200	0.0402	0.0207	0.0808	0.4788
	$k_G(h^{-1})$	0.0742	0.0787	0.0703	0.0951	0.1211

temperature rises to 70 °C, the nucleation rate of cement with silica fume is higher than that of cement with nano-SiO_2. MIX CNCSH has the greatest *N* and *G* values at different elevated temperatures, which confirms the most remarkable effect of nano-C-S-H on cement hydration. The possible reason may be that nano-C-S-H with the largest specific surface area and special surface structures may provide the largest quantity of nucleation sites. However, the quick nucleation may lead to the interdigitation of hydration products which reduces the growing space. This may be the reason for the difference among the increasing rates of nucleation and growth rates for different specimens at different temperatures.

5. Conclusions

This study investigated the hydration kinetics of cement compound system incorporating nanoparticles at elevated temperature. It is a very complicated problem because this system is composed of multi-scale particles with different physicochemical properties. Based on above limited analysis, conclusions can be drawn as the following.

(1) The effect of nanoparticles on cement hydration depends not only on the type of material but also on the temperature. In the investigated temperature conditions of 40 °C–70 °C, addition of 1% nano-$CaCO_3$ has no obvious effect on the process of hydration release heat in comparison to the control sample. However, silica fume, nano-SiO_2 and nano-C-S-H can greatly shorten the induction period at different levels and reduces the arrival time of hydration release heat rate peak. Especially for nano-C-S-H, it not only significantly shortens the induction period of cement hydration but also increases the value of heat release rate peak.

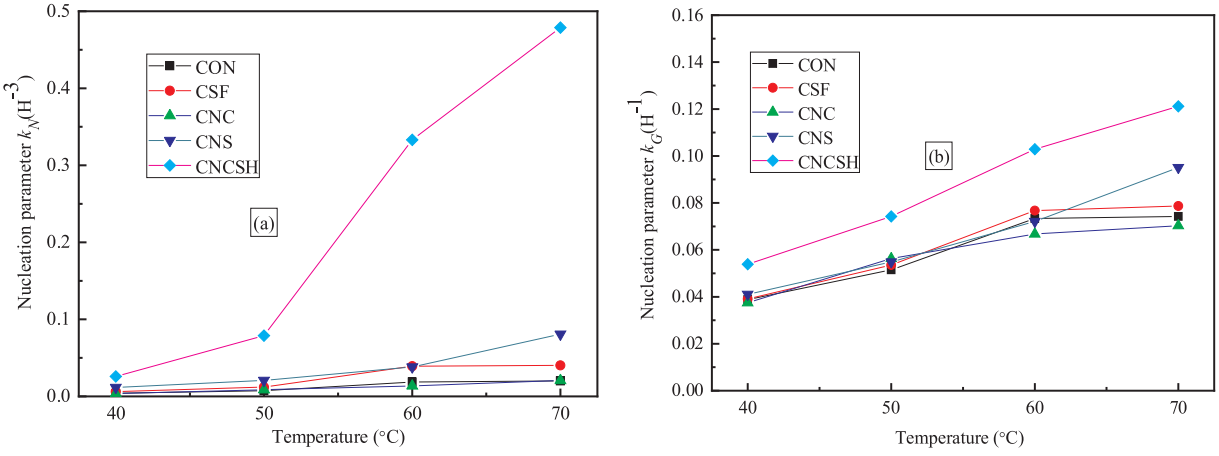

Fig. 11. The relationships of fitted parameters kN and kG with temperature for different specimens.

Table 4
The calculated nucleation and growth rates of cement-based materials.

Temperature (°C)	Parameter	CON	CSF	CNC	CNS	CNCSH
40	$N(um^{-2}h^{-1})$	3.1745	4.6492	3.1043	8.0532	10.4151
	G(um/h)	0.0162	0.0354	0.0339	0.0371	0.0487
50	$N(um^{-2}h^{-1})$	3.2087	4.9541	3.1797	8.0703	16.7314
	G(um/h)	0.0466	0.0484	0.0509	0.0496	0.0671
60	$N(um^{-2}h^{-1})$	4.0797	7.7778	3.5616	8.5711	26.5039
	G(um/h)	0.0663	0.0694	0.0604	0.0652	0.0930
70	$N(um^{-2}h^{-1})$	4.2486	14.8393	4.8807	10.4368	38.1013
	G(um/h)	0.0671	0.0712	0.0636	0.0860	0.1096

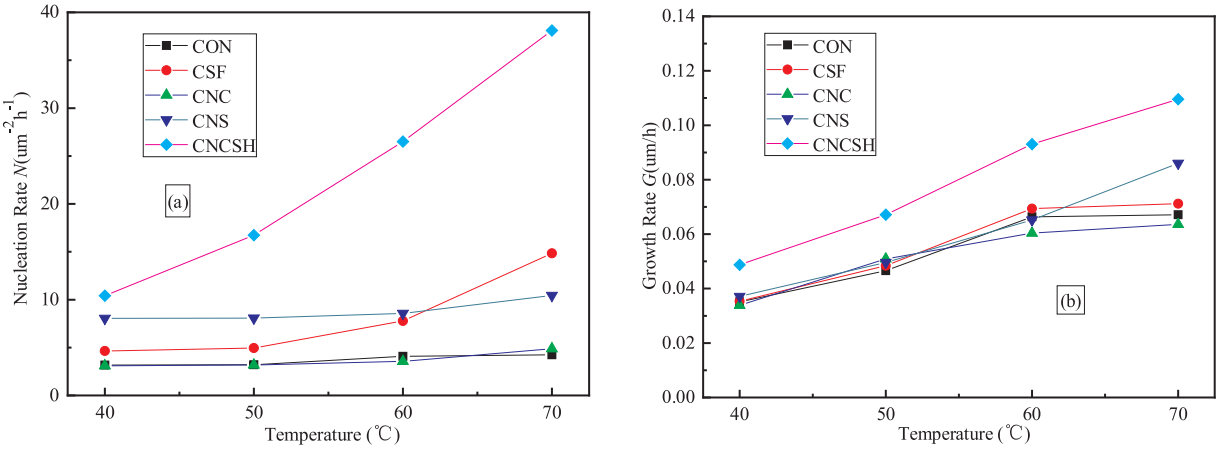

Fig. 12. The relationships of parameters N and G with temperature for different specimens.

(2) The kinetics model employed can describe the nucleation and growth processes of hydrates for cement composites. The simulated results of the acceleration period is more precise than the deceleration and steady periods. During the later deceleration period and total steady period, the simulated heat release rates are mainly higher than the measures results. The possible reason is that both the addition of nanoparticles and elevated temperatures can make the production of hydrates layer in advance.

(3) Addition of 1% nano-SiO_2 particles into cement system can remarkably increase nucleation rate of hydration products at different temperatures. And the nano-C-S-H increases the nucleation and growth rates, and the increase degree of the nucleation rate is much greater than that of the growth rate. However, nano-$CaCO_3$ seems to no obvious effect on the nucleation rate and growth rate of hydration product of cement system. The possible reason for this phenomenon may be the difference in the chemical activity of different nanoparticles.

(4) The effects of nanoparticles on hydration kinetics of cement system at elevated temperatures may be attributed to the synthetic action of chemical activity, affinity and size of nanoparticles. The effect of nano-$CaCO_3$ with low chemical activity or even inert on cement hydration kinetic was eliminated by high sensitivity of cement hydration reaction on temperature.

Acknowledgment

Authors would like to acknowledge the National Natural Science Foundation of China, Grants No. 51678568 and U1534207.

References

[1] N. Hu, G.L. Dai, B. Yan, K. Liu, Recent development of design and construction of medium and long span high-speed railway bridges in China, Eng. Struct. 74 (2014) 233–241.
[2] W. Liu, H. Lund, B.V. Mathiesen, Modelling the transport system in China and evaluating the current strategies towards the sustainable transport development, Energy. Policy 58 (2013) 347–357.
[3] M. Jerman, V. Tydlitát, M. Keppert, M. Čáchová, R. Černý, Characterization of early-age hydration processes in lime-ceramic binders using isothermal calorimetry, x-ray diffraction and scanning electron microscopy, Thermochim. Acta 633 (2016) 108–115.
[4] G.C. Long, M. Wang, Y.J. Xie, K. Ma, Experimental investigation on dynamic mechanical characteristics and microstructure of steam-cured concrete, Sci. China Technol. Sci. 57 (10) (2014) 1902–1908.
[5] D.W.S. Ho, C.W. Chua, C.T. Tam, Steam-cured concrete incorporating mineral admixtures, Cem. Concr. Res. 33 (4) (2003) 595–601.
[6] M. Gesoğlu, Influence of steam curing on the properties of concretes incorporating metakaolin and silica fume, Mater. Struct. 43 (8) (2010) 1123–1134.
[7] G.C. Long, J.G. Yang, Y.J. Xie, The mechanical characteristics of steam-cured high strength concrete incorporating with lightweight aggregate, Constru. Build. Mater. 136 (2017) 456–464.
[8] B.J. Liu, Y.J. Xie, J. Li, Influence of steam curing on the compressive strength of concrete containing supplementary cementing materials, Cem. Concr. Res. 35 (5) (2005) 994–998.
[9] R. Barbarulo, H. Peycelon, S. Prené, J. Marchand, Delayed ettringite formation symptoms on mortars induced by high temperature due to cement heat of hydration or late thermal cycle, Cem. Concr. Res. 35 (1) (2005) 125–131.
[10] X.Y. Wang, H.S. Lee, Modeling the hydration of concrete incorporating fly ash or slag, Cem. Concr. Res. 40 (7) (2010) 984–996.
[11] M. Narmluk, T. Nawa, Effect of fly ash on the kinetics of Portland cement hydration at different curing temperatures, Cem. Concr. Res 41 (6) (2011) 579–589.
[12] L. Mo, M. Liu, A. Al-Tabbaa, M. Deng, W.Y. Lau, Deformation and mechanical properties of quaternary blended cements containing ground granulated blast furnace slag, fly ash and magnesia, Cem. Concr. Res. 71 (2015) 7–13.
[13] W. Saengsoy, T. Nawa, P. Termkhajornkit, Influence of relative humidity on compressive strength of fly ash cement paste, J. Struct. Constr. Eng. 73 (2008) 1433–1441.
[14] L. Senff, D. Hotza, S. Lucas, V.M. Ferreira, J.A. Labrincha, Effect of nano-SiO2 and nano-TiO2 addition on the rheological behavior and the hardened properties of cement mortars, Mater. Sci. Eng. A 532 (2012) 354–361.
[15] M. Oltulu, R. Şahin, Effect of nano-SiO2, nano-Al2O3 and nano-Fe2O3 powders on compressive strengths and capillary water absorption of cement mortar containing fly ash: a comparative study, Energy Build. 58 (2013) 292–301.
[16] S. Kawashima, P. Hou, D.J. Corr, S.P. Shah, Modification of cement-based materials with nanoparticles, Cem. Concr. Compos. 36 (2013) 8–15.
[17] F.H. Han, X.J. He, Z.Q. Zhang, J.H. Liu, Hydration heat of slag or fly ash in the composite binder at different temperatures, Thermochim. Acta. 655 (2017) 202–210.
[18] C. Sonat, C. Unluer, Investigation of the performance and thermal decomposition of MgO and MgO-SiO2 formulations, Thermochimica. Acta. 655 (2017) 251–261.
[19] S. Chuah, Z. Pan, J.G. Sanjayan, et al., Nano reinforced cement and concrete composites and new perspective from graphene oxide, Constr. Build. Mater. 73 (2014) 113–124.
[20] M. Avrami, Kinetics of phase change. ii transformation-time relations for random

distribution of nuclei, J. Chem. Phys. 8 (1940) 212–224.
[21] J.W. Cahn, The kinetics of grain boundary nucleated reactions, Acta Metall. 4 (1956) 449–459.
[22] G.W. Scherer, J. Zhang, J.J. Thomas, Nucleation and growth models for hydration of cement, Cem. Concr. Res. 42 (2012) 982–993.
[23] G. Artioli, J.W. Bullard, Cement hydration: the role of adsorption and crystal growth, Cryst. Res. Technol. 48 (10) (2013) 903–918.
[24] L. Xu, K. Wu, C. Rößler, P. Wang, H.M. Ludwig, Influence of curing temperatures on the hydration of calcium aluminate cement/Portland cement/calcium sulfate blends, Cem. Concr. Res. 80 (2017) 298–306.
[25] B. Lothenbach, K. Scrivener, R.D. Hooton, Supplementary cementitious materials, Cem. Concr. Res. 41 (12) (2011) 1244–1256.